Absence of Metallicity in K-doped Picene: Importance of Electronic Correlations

Andreas Ruff, Michael Sing, and Ralph Claessen

Physikalisches Institut, Universität Würzburg, Am Hubland, 97074 Würzburg, Germany

Hunpyo Lee, Milan Tomić, Harald O. Jeschke, and Roser Valentí

Institut für Theoretische Physik, Goethe-Universität Frankfurt, 60438 Frankfurt am Main, Germany

Potassium-doped picene ($K_x$picene) has recently been reported to be a superconductor at $x = 3$ with critical temperatures up to 18 K. Here we study the electronic structure of K-doped picene films by photoelectron spectroscopy and *ab initio* density functional theory combined with dynamical mean-field theory (DFT + DMFT). Experimentally we observe that, except for spurious spectral weight due to the lack of a homogeneous chemical potential at low K concentrations ($x \approx 1$), the spectra always display a finite energy gap. This result is supported by our DFT + DMFT calculations which provide clear evidence that $K_x$picene is a Mott insulator for integer doping concentrations $x = 1$, 2, and 3. We discuss various scenarios to understand the discrepancies with previous reports of superconductivity and metallic behavior.

Since the discovery of superconductivity in layered organic charge transfer salts in the late 1970s [1], a large variety of organic superconductors have been reported with critical temperatures ranging from a few kelvins to values as high as 38 K in the case of alkali-metal-doped fullerenes [2]. Whether superconductivity is driven by electron-phonon interactions or by electronic correlations has been a subject of intense debate in the last decade, and indeed a significant fraction of these systems are presently being discussed as correlated materials [3,4]. Recently, a pronounced Meissner-Ochsenfeld effect indicating a transition temperature of 18 K was observed in polycrystalline powder samples of potassium-doped picene [5]. Moreover, the recent observation of zero resistivity below 7 K supports these findings [6]. The parent compound picene is a wide band-gap semiconductor (gap ~ 3.3 eV [7]) consisting of planar molecules with five aromatic benzene rings (see inset in Fig. 1). The observation of superconductivity upon K intercalation has also been reported in other aromatic semiconductors, viz., phenanthrene, coronene, and dibenzopentacene [8–10].

In a simple one-electron picture, K intercalation is expected to induce electron transfer into the lowest unoccupied molecular orbital (LUMO) of picene, leading to a partially filled, i.e., metallic conduction band which at low temperatures would host the superconductivity, as suggested in various theoretical studies [9,11–19]. However, such calculations include electronic correlations only at the level of the exchange-correlation functional considered within density functional theory (DFT) and neglect electron-phonon interactions. Both effects can be quite pronounced in molecular solids [20]. In fact, the importance of electron-electron correlations in K_3picene was pointed out by Giovannetti *et al.* [21] and Kim *et al.* [22] who found an

insulating state with antiferromagnetic order from *ab initio* calculations. Experimentally, the picture of the electronic structure has remained controversial: while one photoemission study reported the appearance of metallic spectral weight at the Fermi level for $x = 1$ [23], other authors [24,25] failed to observe a metallic Fermi edge for a wide concentration range from $x = 0.22$ to 3.6 and speculated about the possible role of correlations and polaronic effects [24].

In view of this unsettled situation we have investigated the electronic structure of $K_x$picene in a joint experimental and theoretical effort. For this purpose, extensive photoemission measurements on pristine and potassium-doped picene films have been perfomed, accompanied by *ab initio* density functional theory (DFT) calculations in combination with dynamical mean field theory (DFT + DMFT). Contrary to the results of Ref. [23], both experimental and theoretical results confirm the absence of metallic behavior for any composition of $K_x$picene with integer $x = 1$, 2, 3. This insulating behavior is attributed to strong on-site (i.e., intramolecular) correlations as inferred from an analysis of the DFT + DMFT calculations.

Picene films have been grown in ultrahigh vacuum by thermal evaporation out of a Knudsen cell on clean natively oxidized Si substrates. Subsequent doping was achieved by evaporation of potassium from commercial SAES® dispensers onto the picene films at room temperature. *In situ* photoemission spectra were recorded at room temperature with a total energy resolution of 0.1 and 0.7 eV using He I (21.2 eV) and monochromatized Al $K\alpha$ (1486.6 eV) radiation for valence band and core level spectroscopy, respectively. All experiments have been performed at a base pressure of 1×10^{-10} mbar, which during picene and K deposition did not rise above 5×10^{-9} mbar
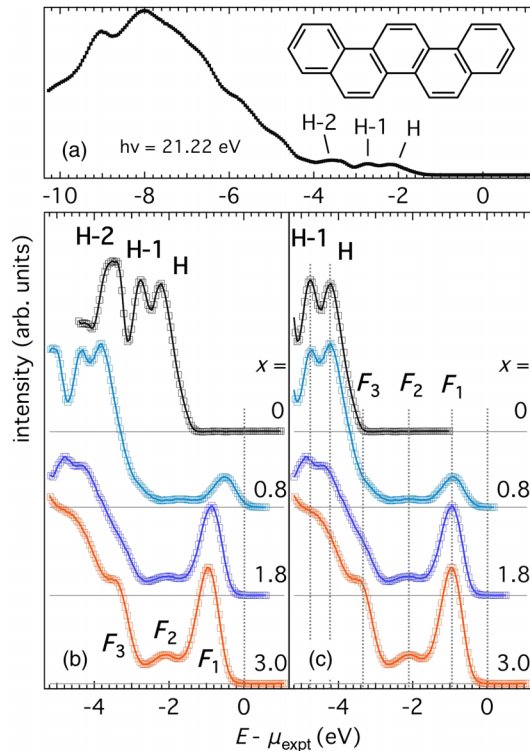
FIG. 1 (color online). (a) Valence band spectrum of a pristine picene film. H, H-1, and H-2 label the highest occupied molecular orbitals of the pristine film. (b) Low-energy part of the valence band spectrum showing the evolution with K doping for various near-integer concentrations. The doping-induced features in the former band gap are assigned by F_1, F_2, and F_3. All energies as measured relative to the experimental Fermi energy μ_{expt}. (c) Same spectra, but energetically aligned at the spectral features of the $x = 3$ spectrum, for which the existence of an equilibrium chemical potential can safely be assumed (see text for details).

and 8×10^{-10} mbar, respectively. The relative intensity of the C1s and K2p core levels was used to determine the doping concentration (also see Supplemental Material [26]). All valence band spectra have been corrected for He Iβ satellite emission.

Bulk picene crystallizes in a monoclinic unit cell with the molecules arranged in a herringbone structure [27]. As typical for planar molecules on inert substrates, our picene films grow in a 3D island mode (Vollmer-Weber-type growth), with the long axis standing out from the surface in order to minimize film-substrate interaction. The c-axis parameter determined from x-ray diffraction is 13.51 Å, very close to its value in bulk material [5,27] (see Supplemental Material [26] for further information). Because of strong K oxidation under ambient atmosphere, we have not been able to measure reliable structural parameters for the K-doped films.

On the theoretical side the crystal structure of K$_x$picene ($x = 1, 2, 3$) has been determined by structural relaxation within DFT using the generalized gradient approximation

(GGA). The projector augmented wave basis was used as implemented in VASP [28–31], with additional van der Waals corrections included in the relaxation process. The subsequent analysis of the electronic structure was performed with the full potential local orbital code FPLO [32].

Figure 1(a) shows the valence band spectrum of a pristine picene film. It is fully consistent with previous photoemission studies [12,23,33], with the highest occupied molecular orbital (HOMO) and following bands clearly resolved at -2.2 (H), -2.8 (H-1) and -3.5 eV (H-2) relative to the experimental Fermi energy (μ_{expt}, determined by the Fermi cut-off of a sputtered gold foil). Figure 1(b) displays the evolution of the spectra with K doping from $x = 0$ to 3 as measured. In agreement with previous work, the doping results in additional features (F_1, F_2, F_3) in the former band gap and an apparent shift of the overall valence band to higher binding energies. This shift is also seen in the C1s core level spectrum (not shown here).

We first discuss the origin of the additional spectral features. In analogy to other alkali-metal-doped organic semiconductors [34,35] F_3 is assigned to the relaxed HOMO, induced by the structural distortion experienced by the doped picene molecules. Its intensity clearly increases with doping, while the strongly decreasing (but still visible) contribution of the H and H-1 peaks in Fig. 1 reflects the diminishing fraction of uncharged molecules upon doping. The weak feature F_2 can be shown to result from the oxidation of surface K atoms with oxygen present in the residual gas of the ultrahigh vacuum system [36,37]. Therefore, it is a purely extrinsic structure not relevant for the following discussions. Finally, the most prominent in-gap feature F_1 is attributed to a (non-rigid-band-like) filling of the former LUMOs, as suggested by the theoretical calculations discussed below.

Next we turn to the evolution of the apparent binding energies in the valence band spectra. Figure 1(b) shows that for $x = 0.8$ the new peak F_1 sits very close or even at the experimental Fermi level, reminiscent of the spectrum reported by Okazaki *et al.* [23] for $x = 1$, while for larger doping concentration it clearly moves away from μ_{expt}, leaving a (half)gap of ≈ 0.5 eV. However, the near-Fermi level position of F_1 around $x = 1$ should not be mistaken for a metallic Fermi edge. First of all, its spectral onset is far too broad to account for a sharp Fermi edge, even considering thermal and instrumental broadening. Moreover, for smaller concentrations between $x = 0$ and 1 the spectral weight of peak F_1 is even observed *well above* the experimental Fermi energy (see Fig. S2 in the Supplemental Material [26]). Such curious behavior was observed also in other alkali-metal-doped organic semiconductor films and was established to result from a lack of thermodynamic equilibrium originating from the weak intermolecular van der Waals coupling [35]. In such a situation, charge fluctuations are strongly suppressed,

thereby preventing the formation of a well-defined chemical potential. The ionic charge transfer induced by alkali-metal doping restores the equilibrium. Because in our case the doping is achieved by K evaporation *after* film growth, the doping concentration will decrease from surface to substrate (note that the x values determined from core level spectroscopy are only valid for a thin surface layer given by the photoemission probing depth of a few nm). Only for sufficiently strong overall doping, full equilibrium within the organic film and between film and substrate is achieved.

In our case we observe saturation of the doping-induced energy shifts at $x \approx 3$, which we identify with equilibrium, i.e., the energies of the $x = 3$ spectrum can be safely referred to the experimental Fermi energy. Consequently, we display in Fig. 1(c) all spectra aligned at the position of the unrelaxed H and H-1 peaks of the $x = 3$ film, which incidentally fixes also the doping-induced features at constant energies. This representation nicely shows the evolution of in-gap spectral weight upon doping, with none of the spectra displaying any metallic Fermi edge. The observation that even the $x = 3$ phase, for which superconductivity has been claimed, remains gapped is most surprising, but in agreement with two previous reports [24,25]. Polaronic effects have been suggested as one possible explanation [24], which may cause a pseudogap at the Fermi level as has been observed, e.g., in oxides [38]. However, such a pseudogap typically exhibits an exponential decay towards the Fermi energy [39], which is not consistent with the present observation. Alternatively, the gap may originate from strong electronic correlations. In fact, in a Hubbard model-type description the intra-molecular Coulomb energy U in organic solids is often comparable or even larger than the bandwidth from inter-molecular hopping [20,40], which can drive partially filled bands into a Mott insulating state.

In order to further explore the latter scenario, we have studied the electronic properties of the DFT-relaxed crystal structures of $K_x$picene ($x = 1, 2, 3$) by a combination of DFT + DMFT calculations, which include correlation effects beyond the GGA approximation in DFT. We start first with the DOS for pristine and $K_x$picene obtained within GGA [Figs. 2(a), 2(b), 2(d), and 2(f)]. We observe a metallic state for odd x as well as a band gap for $x = 2$, consistent with previous DFT calculations.

In DFT + DMFT the kinetic part H_K of the Hamiltonian [Eq. (1)] is obtained from the DFT calculations by considering the tight-binding approach. Since the DFT results indicate some hybridization between the bands derived from LUMO and LUMO + 1 of the pristine picene molecules, we consider for the DMFT calculations a two-orbital Hubbard model with a Coulomb interaction U and Hund's coupling J_z as well as on-site hopping parameters $t_\perp$ between molecular orbitals on the same site. The Hamiltonian we solve is $H = H_K + H_I$ where
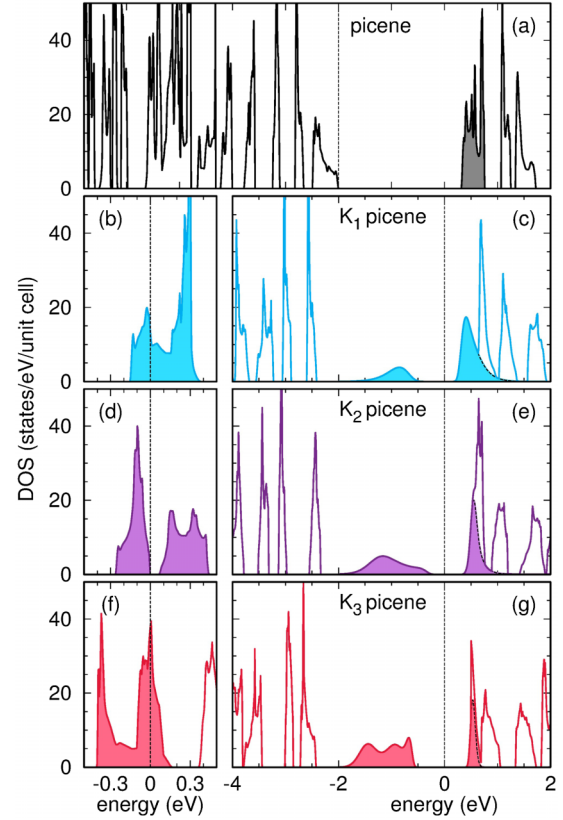

FIG. 2 (color online). Density of states of pristine and K-doped picene. (a) DFT DOS for pristine picene with the part of the spectrum arising from LUMO and LUMO + 1 levels of picene marked by gray shading. (b), (d), (f) DFT DOS of the region close to the Fermi level for K_1picene, K_2picene, and K_3picene, respectively. (c), (e) and (g) Combined DFT + DMFT DOS of the same compounds. For details see text.

$$H_K = -\sum_{\langle ij\rangle m\sigma} t_{ij}^m c_{mj\sigma}^\dagger c_{mi\sigma} - t_\perp \sum_{i\sigma} c_{1i\sigma}^\dagger c_{2i\sigma}$$

$$H_I = U\sum_{mi} n_{mi\uparrow}n_{mi\downarrow} + \sum_\sigma [(U - 2J_z)n_{1i\sigma}n_{2i\bar\sigma} \qquad (1)$$

$$+ (U - 3J_z)n_{1i\sigma}n_{2i\sigma}],$$

i, j denote sites and the sum $\langle ij\rangle$ runs over all sites and m denotes molecular orbitals. Bands which are away from the Fermi level are not expected to be significantly renormalized by correlations, and we save on computational effort by ignoring them in the DMFT calculation. As an impurity solver for the DMFT equations, we employed the weak-coupling continuous time quantum Monte Carlo. Our results are for $T = 0.025$ eV, $U = 1.6$ eV, and $J_z = U/8$. This choice of interaction parameters was guided by recent quantum chemistry [21] and constrained random phase approximation (cRPA) estimates [40]. Note that for K_3picene, we find the metal-insulator transition between $U = 0.6$ eV (metallic) and $U = 0.8$ eV (insulating). The analytic continuation of the converged impurity Green's function to real frequencies was performed with the

maximum entropy method. The resulting spectral function for these two orbitals is shown in Fig. 2, embedded into the DFT-DOS of the noninteracting bands.

Clearly, the DMFT spectral functions show a Mott gap not only for doping levels of $x = 1$ and $x = 3$, but also for $x = 2$ which in bare DFT is a band insulator with a small gap. A closer look at the DOS [Fig. 3(b)] of K_2picene shows that—contrary to the expectation of a filled picene LUMO derived band and an empty picene LUMO + 1 derived band—a Mott gap opens in *both* orbitals. Interestingly, energy positions and gap size do not seem to depend much on the actual doping level, except for the spectral weight transfer from upper to lower Hubbard bands, and correspond favorably with the experimental spectra, except for some fine structure at higher x not resolved in photoemission. The origin of the Mott gap for $K_x$picene with $x = 1, 2, 3$ lies not only in the on-site Coulomb interaction U and the Hund's coupling J_z but also in the interorbital hybridization $t_\perp$. We would like to note that our calculations did neither include electron-phonon effects, which may reduce the Hubbard interaction, as was shown by Sangiovanni *et al.* [41], nor magnetic ordering, where the possibility of a Mott insulator in the antiferromagnetic state could be investigated, as was found by the authors of Refs. [21,22] by performing *ab initio* DFT calculations. This will be a subject of future work.

Both experiment and theory thus arrive at the same conclusion that $K_x$picene films are (Mott-)insulating for all compositions with integer x, including the n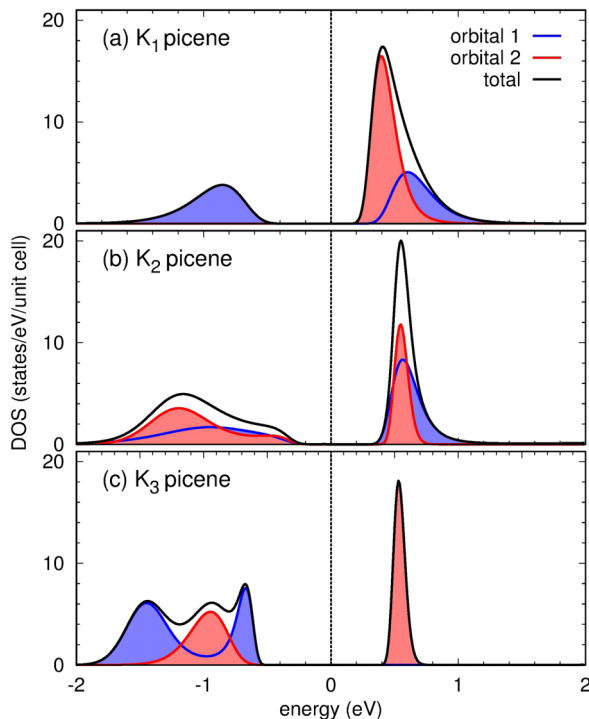ominally superconducting phase $x = 3$. This leaves two open questions: (1) What is the electronic ground state for *noninteger* x, and (2) how can the insulating behavior of the $x = 3$ phase be reconciled with the reports on superconductivity?

Concerning the first question we note that in a Mott-insulator deviation from integer band filling is normally expected to lead to a metallic phase with electron- or hole-type carriers [42]. Note, however, that the doping concentration determined in our photoemission experiments is a macroscopic quantity, averaged over the extension of the photon spot (~ 1 mm), and may be composed of phase-separated integer-filled domains. In fact, a recent Raman study [43] has observed that $K_x$picene decomposes into $x = 0, 2$, and 3 phases, while a defined $x = 1$ signal could not be detected, indicating that this phase is not stable. One can thus understand the photoemission spectra as a superposition of different integer x phases. Because the shape and gapped behavior of the corresponding theoretical spectra is very similar, the main doping effect will consist in the appearance and increasing spectral weight of the LUMO and LUMO + 1 derived lower Hubbard band, as indeed reflected by the behavior of feature F_1 in our experimental spectra.

The second question is more puzzling. Our present results are in line with the general observation that alkali-metal-doped organic semiconductors are mostly insulating [35,44], with K-doped fullerene (K_3C_{60}) being one of the rare exceptions [45]. On the other hand, in the original paper by Mitsuhashi *et al.* it has been reported that in $K_{2.9}$picene the diamagnetic (i.e., superconducting) phase is reached from a Pauli paramagnetic, hence *metallic* phase [5]. This is also supported by the resistivity measurements by Teranishi *et al.* [6]. Reconciling our room-temperature results with these observations would require an insulator-to-metal transition somewhere between 300 and 25 K (the highest measured temperature in Ref. [5]). The Mott-Hubbard scenario derived from our DFT + DMFT calculations does not provide any mechanism for such a transition but would rather stabilize the gap towards low temperatures. Moreover, we do not observe any indications for metallicity down to 40 K in our photoemission study (not shown).

Another important aspect is that so far all superconducting signatures have been obtained from intercalated compact picene powder [5,43], in contrast to the *in vacuo* grown thin films used here. It is possible that both sets of samples differ in subtle structural details accounting for the conflicting findings. On the other hand, the DFT + DMFT calculations are based on a DFT-relaxed *bulk* structure which one would expect to be relevant for the polycrystalline powder, at least for the interior of the powder grains. It is thus tempting to speculate about the possibility of the superconducting phase actually being located at the grain boundaries, which may have structural and/or electronic properties different from the bulk. Certainly more clarifying work needs to be done in this direction.

FIG. 3 (color online). Orbital resolved and total DMFT spectral functions of (a) K_1picene, (b) K_2picene, and (c) K_3picene.

In summary, our combined photoemission and DFT + DMFT study finds that $K_x$picene is a correlated Mott insulator for any integer doping concentration $x = 1$, 2, and 3. The insulating behavior of samples with macroscopic noninteger filling observed in the experiment is attributed to microscopic phase separation in line with recent Raman results. The apparent spectral weight at or even above the Fermi level experimentally observed for low doping ($x \lesssim 1$) is attributed to a lack of thermodynamical equilibrium, resulting from weak intermolecular van der Waals interactions. The resulting discrepancy between the Mott-insulating behavior of particularly K_3picene found here and the recent reports of superconducting signatures [5,6] calls for further investigations.

[1] N. Toyota, M. Lang, and J. Müller, *Low-Dimensional Molecular Metals* (Springer-Verlag, Berlin Heidelberg, 2007).
[2] T. Palstra, O. Zhou, Y. Iwasa, P. Sulewski, R. Fleming, and B. Zegarski, Solid State Commun. **93**, 327 (1995).
[3] M. Capone, M. Fabrizio, C. Castellani, and E. Tosatti, Science **296**, 2364 (2002).
[4] B. Powell and R. McKenzie, Rep. Prog. Phys. **74**, 056501 (2011).
[5] R. Mitsuhashi, Y. Suzuki, Y. Yamanari, H. Mitamura, T. Kambe, N. Ikeda, H. Okamoto, A. Fujiwara, M. Yamaji, and N. Kawasaki et al., Nature (London) **464**, 76 (2010).
[6] K. Teranishi, X. He, Y. Sakai, M. Izumi, H. Goto, R. Eguchi, Y. Takabayashi, T. Kambe, and Y. Kubozono, Phys. Rev. B **87**, 060505(R) (2013).
[7] H. Okamoto, N. Kawasaki, Y. Kaji, Y. Kubozono, A. Fujiwara, and M. Yamaji, J. Am. Chem. Soc. **130**, 10470 (2008).
[8] X. Wang, R. Liu, Z. Gui, Y. Xie, Y. Yan, J. Ying, X. Luo, and X. Chen, Nat. Commun. **2**, 507 (2011).
[9] Y. Kubozono et al., Phys. Chem. Chem. Phys. **13**, 16476 (2011).
[10] M. Xue, T. Cao, D. Wang, Y. Wu, H. Yang, X. Dong, J. He, F. Li, and G. Chen, Sci. Rep. **2**, 389 (2012).
[11] T. Kosugi, T. Miyake, S. Ishibashi, R. Arita, and H. Aoki, J. Phys. Soc. Jpn. **78**, 113704 (2009).
[12] F. Roth, M. Gatti, P. Cudazzo, M. Grobosch, B. Mahns, B. Büchner, A. Rubio, and M. Knupfer, New J. Phys. **12**, 103036 (2010).
[13] P. L. de Andres, A. Guijarro, and J. A. Vergés, Phys. Rev. B **83**, 245113 (2011).
[14] T. Kosugi, T. Miyake, S. Ishibashi, R. Arita, and H. Aoki, Phys. Rev. B **84**, 214506 (2011).
[15] P. Cudazzo, M. Gatti, F. Roth, B. Mahns, M. Knupfer, and A. Rubio, Phys. Rev. B **84**, 155118 (2011).
[16] A. Subedi and L. Boeri, Phys. Rev. B **84**, 020508(R) (2011).
[17] M. Casula, M. Calandra, G. Profeta, and F. Mauri, Phys. Rev. Lett. **107**, 137006 (2011).
[18] T. Kato, T. Kambe, and Y. Kubozono, Phys. Rev. Lett. **107**, 077001 (2011).
[19] M. Casula, M. Calandra, and F. Mauri, Phys. Rev. B **86**, 075445 (2012).
[20] R. Claessen, M. Sing, U. Schwingenschlögl, P. Blaha, M. Dressel, and C. S. Jacobsen, Phys. Rev. Lett. **88**, 096402 (2002).
[21] G. Giovannetti and M. Capone, Phys. Rev. B **83**, 134508 (2011).
[22] M. Kim, B. I. Min, G. Lee, H. J. Kwon, Y. M. Rhee, and J. H. Shim, Phys. Rev. B **83**, 214510 (2011).
[23] H. Okazaki et al., Phys. Rev. B **82**, 195114 (2010).
[24] B. Mahns, F. Roth, and M. Knupfer, J. Chem. Phys. **136**, 134503 (2012).
[25] M. Caputo et al., J. Phys. Chem. C **116**, 19902 (2012).
[26] See Supplemental Material at http://link.aps.org/supplemental/10.1103/PhysRevLett.110.216403 for details on doping concentration, picene structure, and nonequilibrium behavior.
[27] A. De, R. Gosh, S. Roychowdhury, and P. Roychowdhury, Acta Crystallogr. Sect. C **41**, 907 (1985).
[28] G. Kresse and J. Hafner, Phys. Rev. B **47**, 558 (1993).
[29] G. Kresse and J. Furthmüller, Phys. Rev. B **54**, 11169 (1996).
[30] P. E. Blöchl, Phys. Rev. B **50**, 17953 (1994).
[31] G. Kresse and D. Joubert, Phys. Rev. B **59**, 1758 (1999).
[32] H. Jeschke, M. Tomić, H. Lee, and R. Valentí (to be published).
[33] Q. Xin, S. Duhm, F. Bussolotti, K. Akaike, Y. Kubozono, H. Aoki, T. Kosugi, S. Kera, and N. Ueno, Phys. Rev. Lett. **108**, 226401 (2012).
[34] M. Ramsey, M. Schatzmayr, S. Stafström, and F. Netzer, Europhys. Lett. **28**, 85 (1994).
[35] N. Koch, C. Chan, A. Kahn, and J. Schwartz, Phys. Rev. B **67**, 195330 (2003).
[36] M. Merkel, M. Knupfer, M. S. Golden, J. Fink, R. Seemann, and R. L. Johnson, Phys. Rev. B **47**, 11470 (1993).
[37] A. Ruff, S. Schatz, M. Sing, and R. Claessen (to be published).
[38] D. Schrupp, M. Sing, M. Tsunekawa, H. Fujiwara, S. Kasai, A. Sekiyama, S. Suga, T. Muro, V. Brabers, and R. Claessen, Europhys. Lett. **70**, 789 (2005).
[39] A. S. Alexandrov and J. Ranninger, Phys. Rev. B **45**, 13109 (1992).
[40] Y. Nomura, K. Nakamura, and R. Arita, Phys. Rev. B **85**, 155452 (2012).
[41] G. Sangiovanni, M. Capone, C. Castellani, and M. Grilli, Phys. Rev. Lett. **94**, 026401 (2005).
[42] M. Imada, A. Fujimori, and Y. Tokura, Rev. Mod. Phys. **70**, 1039 (1998).
[43] T. Kambe et al., Phys. Rev. B **86**, 214507 (2012).
[44] G. G. Fuentes and M. Knupfer, Appl. Phys. A **84**, 329 (2006), and references therein.
[45] D. Poirier, Appl. Phys. Lett. **64**, 1356 (1994).